

Reactive Events at the Graphene Oxide-Water Interface

Electronic Supplementary Information

Rolf David^{a,b} and Revati Kumar^{*a}

^aDepartment of Chemistry, Louisiana State University, Baton Rouge, LA 70803, USA

^bCurrent affiliation: PASTEUR, Department of Chemistry, École Normale Supérieure, PSL University, Sorbonne Université, CNRS, 75005 Paris, France

*E-mail: revatik@lsu.edu

Simulation details.....	2
Representation of the simulation boxes	4
Representation of the two graphene oxide sheets.....	5
Hydronium hopping function H(t).....	6
References	7

Simulation details

Two graphene oxide GO sheets were generated based on the work of Sinclair *et al.*,¹ to have a total number of 180 carbons and 44 oxygen groups for GO_{4/1} (for a C/O ratio of 4.09, 24 epoxide groups and 20 hydroxyl groups) or 90 for GO_{2/1} (for a C/O ratio of 2.00, 50 epoxide groups and 40 hydroxyl groups). For each case the GO sheet was placed in contact with 265 water molecules on one side of the sheet, using the packmol software,² generating a solvent layer of approximately 20 Å. Furthermore, the box was extended in the direction perpendicular to the GO-water interface, to include a 70 Å length vacuum/air region above the water layer giving rise to a box dimension of 22.0 Å x 21.2 Å x 104.0 Å. All simulations, both classical molecular dynamics and DFT molecular dynamics were carried out using periodic boundary conditions. While the simulations should really be periodic in only two dimensions (x and y) and non periodic in the z-direction, a quasi 2D periodic boundary condition is achieved using the large vacuum region in the z-direction. In order to generate the initial configurations for the DFT simulations, as previously published,³ each system was first simulated using classical molecular dynamics with the OPLS-AA⁴ force-field for the sheet and SPC/E⁵ water, with PPPM Ewald method⁶ for long range electrostatics (cutoff of 12 Å for the real space terms in the Ewald summation). The SHAKE algorithm⁷ was used to enforce the rigid geometry of the SPC/E waters. After a geometry coupled with a cell minimization, each system was equilibrated for 500 ps (with a timestep of 0.5 fs) in the NVT ensemble at a temperature of 300K and using a Nosé-Hoover thermostat^{8,9} (with a coupling constant of 50 fs⁻¹). Following this a production run for 1 ns was carried out in the NVT ensemble with snapshots extracted every 200 ps. These five snapshots were selected as initial configurations for five DFT simulations for each GO system. All DFT calculations and simulations were carried out using the CP2K program^{10,11} with the revPBE functional^{12,13} + empirical D3 dispersion correction¹⁴ along with the DZVP-MOLOPT-SR¹⁵ basis set and GTH pseudopotentials¹⁶⁻¹⁸. For every snapshot, the system was first subjected to geometry optimization with the LBFGS algorithm.¹⁹ In addition, during geometry optimization the parameters a and b (x- and y-direction respectively) were allowed to relax and the cell dimension in the z-direction (c parameter) was set and kept fixed at 70.0 Å, giving rise to a vacuum layer 40.0 Å thick. This step reduces the strain on the system, mostly by buckling as the cell variations are within

1 Å. In Figure S1 the entire simulation box is represented (x and y cell values are averaged for all starting point of the same oxidation level (with a variation of 0.2 Å). In Figure S2, only the carbons are represented for a better view of the buckling of the sheet, as the cell are very close in value for both GO.sheets, but very different in buckling. A periodic Poisson solver for electrostatics was used. Following this optimizations, each simulations was carried out for a total of 25 ps in the NVT ensemble at 300 K, using Canonical Sampling through Velocity Rescaling (CSVR) thermostat²⁰ with a 100 fs⁻¹ coupling constant. The first 5 ps of each trajectory were taken as equilibration and the remaining 25 ps as production run. From the five simulations for each case, GO_{2/1} and GO_{4/1}, a total of 125 ps (5 x 25 ps) was obtained for each level of oxidation of the GO sheet.

Representation of the simulation boxes

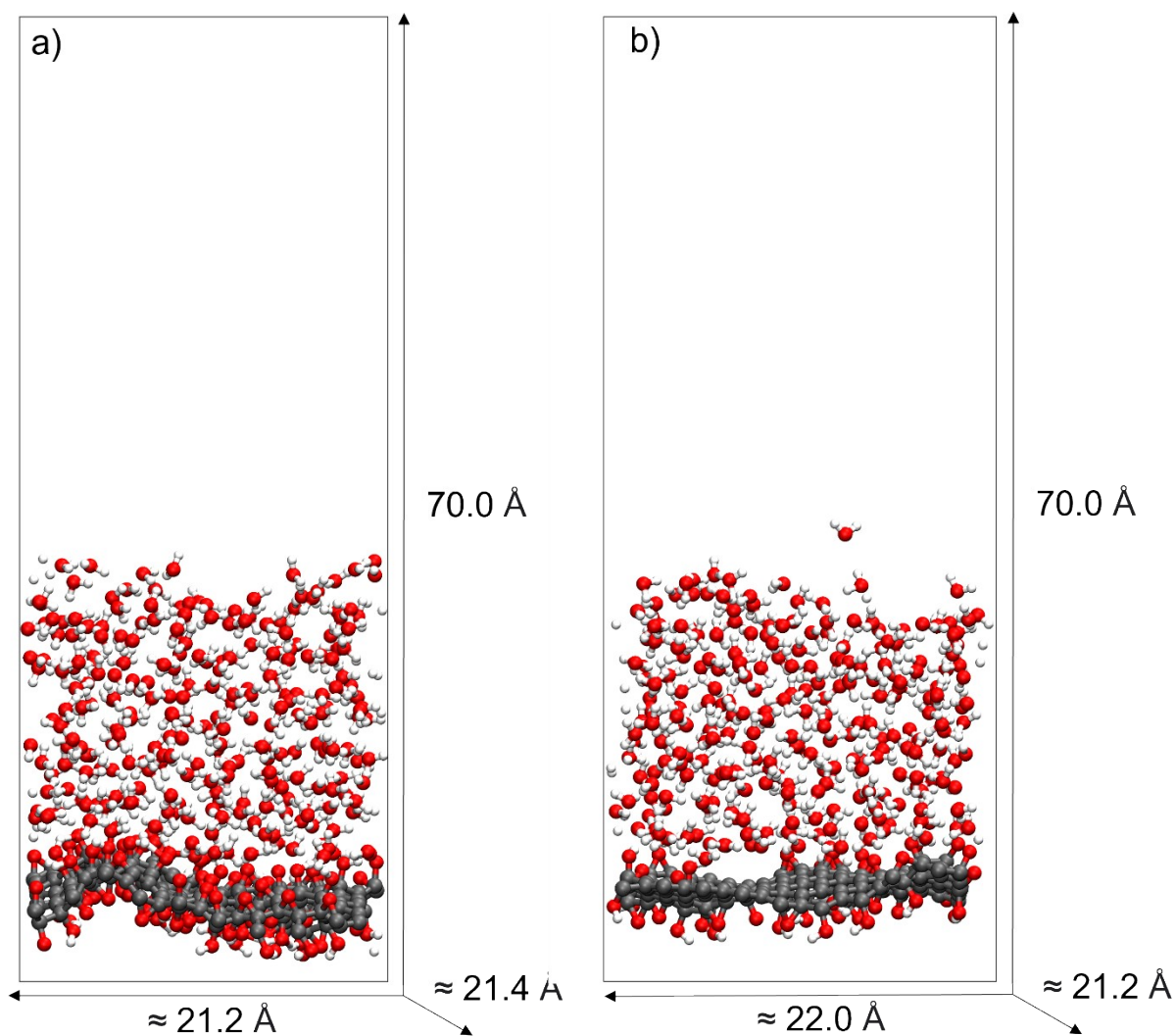
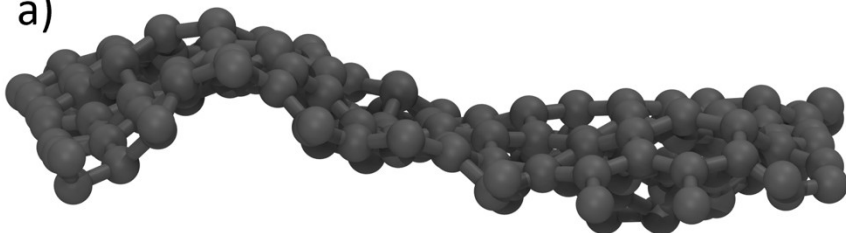


Figure S1. Representation of the simulation boxes with the GO sheet, the water film, and the vacuum layer. a) $GO_{2/1}$ b) $GO_{4/1}$. Carbon, oxygen, and hydrogen are represented in grey, red and white respectively.

Representation of the two graphene oxide sheets

a)



b)

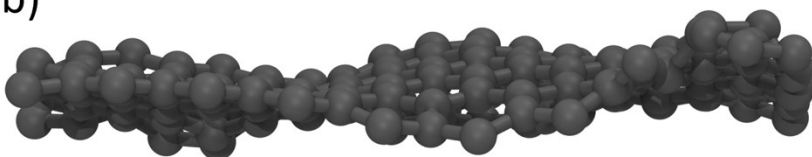


Figure S2: Carbon only representation of the GO sheets to show the difference in buckling. a) GO_{2/1} b) GO_{4/1}

Hydronium hopping function $H(t)$

At each timestep, t , a hydronium is identified (i.e an oxygen atom carrying three hydrogen atoms) and its O atom recorded ($O(t)$).

At t equals 0, $H(0)$ equals 0 (with or without the presence of a hydronium). Only water-water hopping is considered.

For each Δt , the hydronium oxygen is labelled as $O(t + \Delta t)$ and $H(t + \Delta t)$ is calculated as follows :

$H(t + \Delta t) = H(t) + 0$, if the oxygen-carrying the three hydrogen atoms is the same as the one at the previous timestep ($O(t + \Delta t) = O(t)$)

$H(t + \Delta t) = H(t) + 1$, if the oxygen is different than the one at the time t ($O(t + \Delta t) \neq O(t)$) and does not have the same O atom as any of the five previous hydroniums with distinctly different O atoms. If the new hydronium has the O atom that was previously part of the hydronium (going back to up to five previous hydronium O atoms with distinctly different O atoms) then $H(t + \Delta t) = H(t) - m$, where m is 1 if it is the previous O atom, 2 if it is the O atom before that and so on till $m=5$.

In this work, most of the time m is equal to 1 and very rarely equals to 2-3, which is when there is a concerted back-jump or a circular arrangement between waters.

References

- 1 R. C. Sinclair and P. V. Coveney, *J. Chem. Inf. Model.*, 2019, **59**, 2741–2745.
- 2 L. Martínez, R. Andrade, E. G. Birgin and J. M. Martínez, *J. Comput. Chem.*, 2009, **30**, 2157–2164.
- 3 R. David, A. Tuladhar, L. Zhang, C. Arges and R. Kumar, *J. Phys. Chem. B*, 2020, **124**, 8167–8178.
- 4 W. L. Jorgensen, D. S. Maxwell and J. Tirado-Rives, *J. Am. Chem. Soc.*, 1996, **118**, 11225–11236.
- 5 H. J. C. Berendsen, J. R. Grigera and T. P. Straatsma, *J. Phys. Chem.*, 1987, **91**, 6269–6271.
- 6 R. W. Hockney and J. . Eastwood, *Computer Simulation Using Particles*, Taylor & Francis, 1988.
- 7 J.-P. Ryckaert, G. Ciccotti and H. J. . Berendsen, *J. Comput. Phys.*, 1977, **23**, 327–341.
- 8 S. Nosé, *Mol. Phys.*, 1984, **52**, 255–268.
- 9 W. G. Hoover, *Phys. Rev. A*, 1985, **31**, 1695–1697.
- 10 J. VandeVondele, M. Krack, F. Mohamed, M. Parrinello, T. Chassaing and J. Hutter, *Comput. Phys. Commun.*, 2005, **167**, 103–128.
- 11 J. Hutter, M. Iannuzzi, F. Schiffmann and J. VandeVondele, *Wiley Interdiscip. Rev. Comput. Mol. Sci.*, 2014, **4**, 15–25.
- 12 J. P. Perdew, K. Burke and M. Ernzerhof, *Phys. Rev. Lett.*, 1996, **77**, 3865–3868.
- 13 Y. Zhang and W. Yang, *Phys. Rev. Lett.*, 1998, **80**, 890–890.
- 14 S. Grimme, J. Antony, S. Ehrlich and H. Krieg, *J. Chem. Phys.*, 2010, **132**, 154104.
- 15 J. VandeVondele and J. Hutter, *J. Chem. Phys.*, 2007, **127**, 114105.
- 16 S. Goedecker, M. Teter and J. Hutter, *Phys. Rev. B*, 1996, **54**, 1703–1710.
- 17 C. Hartwigsen, S. Goedecker and J. Hutter, *Phys. Rev. B*, 1998, **58**, 3641–3662.
- 18 M. Krack, *Theor. Chem. Acc.*, 2005, **114**, 145–152.
- 19 R. H. Byrd, P. Lu, J. Nocedal and C. Zhu, *SIAM J. Sci. Comput.*, 1995, **16**, 1190–1208.
- 20 G. Bussi, D. Donadio and M. Parrinello, *J. Chem. Phys.*, 2007, **126**, 014101.